npj | climate and atmospheric science

Article

Published in partnership with CECCR at King Abdulaziz University

https://doi.org/10.1038/s41612-024-00805-z

Structural fluctuations of the Arctic Oscillation tied to the Atlantic Multidecadal Oscillation

Hainan Gong[1,2], Kangjie Ma[1,3], Bo Liu[4], Judah Cohen[5,6] & Lin Wang[1,2]

The Arctic Oscillation (AO) has been observed to undergo distinct decadal structural fluctuations that significantly influence regional weather and climate. Understanding the drivers and mechanisms behind the AO's spatial nonstationarity is critical for improving climate predictions related to the AO. We present evidence that the Atlantic Multidecadal Oscillation (AMO) plays a pivotal role in modulating AO's Pacific center in recent decades. The poleward amplified cooling associated with negative AMO enhances the north-south temperature gradient and results the strengthened westerly winds and stratospheric polar vortex (SPV) responses, which reflects more planetary waves from the North Pacific to the North Atlantic. This enhances the atmospheric coupling between these regions and leads to a more pronounced Pacific center within the AO pattern. Numerical simulations from ECHAM5 and 35 CMIP6 models further corroborate the essential role of the AMO. These findings advance our understanding of the mechanisms driving the variability of the AO pattern.

The Arctic Oscillation (AO) is the principal mode of low-frequency atmospheric variability in the extratropical Northern Hemisphere[1]. It is marked by a seesaw pattern of atmospheric pressure between the polar and mid-latitude regions and plays a crucial role in driving the weather and climate in the Northern Hemisphere, particularly during winter[2–16]. Previous studies believed that the annular structure of the AO was generally fixed and unchanging[1–3]. However, the AO's spatial structure of the AO actually varies under certain specific conditions, such as the strength of stratospheric polar vortex (SPV) events[17,18], and these changes can lead to significant differences in AO's impact on regional weather and climate, especially for western North America and East Asia[7,10,19]. For instance, when the AO's Pacific center is strong, it can lead to significant cooling in western North American and widespread warming in East Asia during the positive phase of AO. Conversely, these effects are much weaker when the Pacific center of AO is less pronounced[10,20]. This variability of AO pattern poses a challenge for climate models to capture its spatial dynamics and climate impacts of the AO[19–25].

Understanding the drivers and mechanisms behind the AO's spatial variability, especially for its Pacific center, is essential for refining climate predictions and projections for the western North America and East Asia[10]. Previous studies have found that the winter AO's Pacific center varies over time[8–10] and identified the atmospheric coupling between the North Pacific and North Atlantic as an important factor modulating the winter AO's Pacific center[9,10]. However, it remains unclear which physical processes are responsible for the temporal evolution in the North Pacific-North Atlantic relationship and the consequently variable Pacific center of the AO pattern. In addition, given that large-scale sea surface temperature (SST) variability significantly influences the temporal evolution of atmospheric circulation over multidecadal timescales[26–33], a pivotal question emerges: Could the of the AO's Pacific center affected by the multidecadal variability of these underlying SST forcing? Answering these questions is crucial for elucidating the mechanisms underlying the AO's spatial nonstationarity and enhancing projections of AO-related climate impacts.

By integrating observational data with climate simulations, we aim to provide a comprehensive understanding of the physical processes driving the nonstationarity of AO's Pacific center on multidecadal time scale, especially exploring the role and mechanism of the decadal variations of SPV and Atlantic Multidecadal Oscillation (AMO) SST variability in the multidecadal changes of the AO's Pacific center. This understanding is vital for enhancing our ability to predict and project the impacts of AO-related climate variability on western North America and East Asia, thereby contributing to more effective climate adaptation strategies.

[1]Center for Monsoon System Research, Institute of Atmospheric Physics, Chinese Academy of Sciences, Beijing, China. [2]Collaborative Innovation Center on Forecast and Evaluation of Meteorological Disasters (CIC-FEMD), Nanjing University of Information Science & Technology, Nanjing, China. [3]College of Earth and Planetary Sciences, University of Chinese Academy of Sciences, Beijing, China. [4]CMA Earth System Modeling and Prediction Centre (CEMC), Beijing, China. [5]Atmospheric and Environmental Research, Inc., Lexington, Massachusetts, USA. [6]Department of Civil and Environmental Engineering, Massachusetts Institute of Technology, Cambridge, MA, USA. e-mail: wanglin@mail.iap.ac.cn

Results

Role of SPV on the time-varying AO's Pacific center

Analysis of the AO pattern from the ERA5 dataset over 1958–2022 reveals that it accounts for 32.5% of the total variance in SLP variability across the extratropical Northern Hemisphere. It features an anomalous low-pressure center over the Arctic with two high-pressure centers over the North Pacific and North Atlantic (Supplementary Fig. 1a). This large-scale atmospheric circulation anomaly significantly influences surface air temperature (SAT) changes, especially land SATs in the Northern Hemisphere[11–16]. A positive AO phase correlates with warming in northern Eurasia and southeastern North America and cooling in Greenland and northern Africa (Supplementary Fig. 1b).

It is noted that similar to the AO index, which displays low-frequency fluctuations from 1958 to 2022 (Supplementary Fig. 1c), the AO pattern-particularly the Pacific center-has also experienced significant changes during this period. Figure 1a illustrates the temporal fluctuation of the Pacific center intensity of AO (PCI) during the winters from 1958–2022. We observed significant multidecadal variations in the PCI, with low amplitude prior to 1980 and peak amplitude between 1980 and 2000, and a subsequent marked decline post-2000. We find that these changes in the PCI are closely aligned with the multidecadal oscillations in the strength of SPV (Fig. 1a), suggesting, that a larger amplitude of the PCI is associated with a stronger SPV during 1958–2022. Notably, the correlation coefficient between the sliding SPV and PCI is 0.88, exceeding 99% confidence level, indicating a robust relationship.

To elucidate the physical processes of the SPV influencing the PCI during more recent decades, we specifically analyze two distinct 21-year periods: one with strong SPV and PCI from 1980 to 2000 (SSPV), and another with weak SPV and PCI from 2000 to 2020 (WSPV). During SSPV, the stratospheric polar jet stream was notably stronger than during WSPV. According to planetary wave propagation theory[34], the strength of the westerlies associated with the SPV in winter dictates the upward

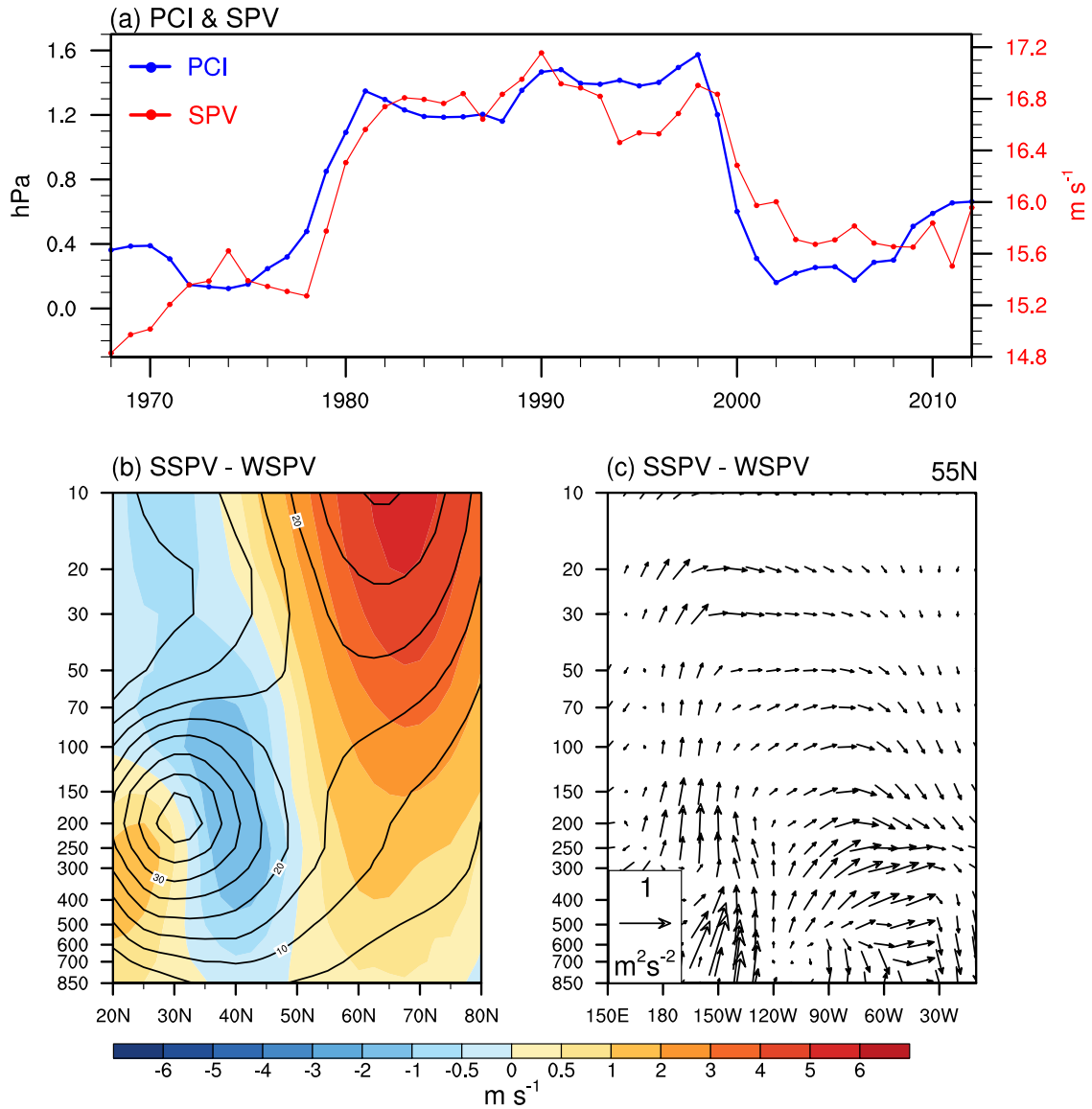

Fig. 1 | Stratospheric polar vortex (SPV) governing the Pacific center of AO. **a** Time-varying Pacific center intensity in winter AO pattern (PCI, blue dotted line) and stratospheric polar vortex (SPV, red dotted line) in a 21-year sliding window during winters 1958–2022 in ERA5 dataset. The PCI is obtained by the SLP anomalies regressed onto the 21-year sliding AO index which have been pre-smoothed using 3-year running averages. **b** The differences of zonal-mean zonal wind (shading) between strong SPV (SSPV) period (1980–2000) and weak SPV (WSPV) period (2000-2020). Contours indicate the climatology of winter mean zonal-mean zonal wind during 1958–2022. **c** The differences in wave activity fluxes along 55°N between SSPV and WSPV periods. The vertical component is multiplied by 1×10^4.

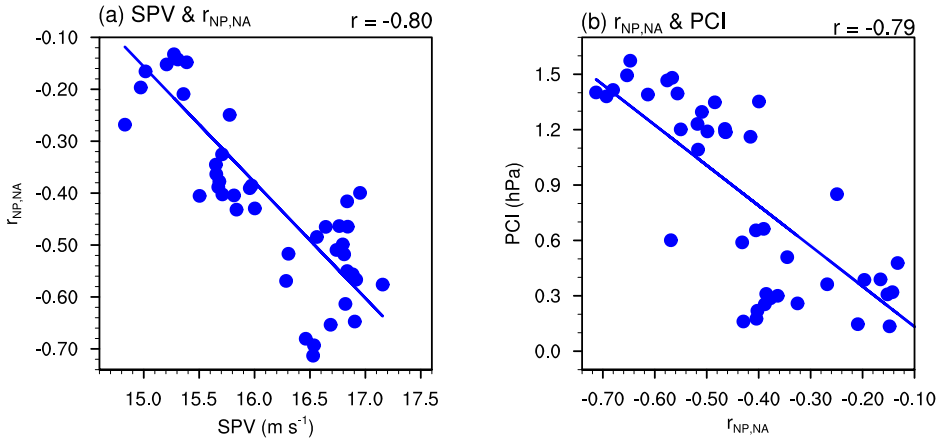

Fig. 2 | Relationship of the SPV and North Pacific-North Atlantic coupling ($r_{NP,NA}$) with the intensity of AO's centers. a Scatterplot of sliding $r_{NP,NA}$ and the SPV in a 21-year window during winters 1958–2022. **b** As in **a**, but for the PCI and $r_{NP,NA}$.

propagation and downward reflection of planetary waves at mid-to-high latitudes[17,18,20]. Consequently, the enhanced westerlies during SSPV, extending from the upper troposphere to the stratosphere (Fig. 1b), facilitate the reflection of planetary waves that typically propagate vertically from the North Pacific into the North Atlantic (Fig. 1c). This dynamical process significantly intensifies the atmospheric coupling between the North Pacific and North Atlantic, evidenced by a strong negative correlation ($r = -0.8$) between the relationship of SLP variability in these regions (denoted as $r_{NP,NA}$, also referred to as the Aleutian Low and Icelandic Low seesaw[9,35,36]) and the magnitude of SPV (Fig. 2a).

Given that AO variability is intrinsically rooted from the North Atlantic dynamics[2,4,10], the intensified North Pacific-North Atlantic coupling during SSPV contributes to an enhanced involvement of North Pacific variability in the overall AO pattern, markedly intensifying the PCI compared to the WSPV period (Supplementary Fig. 2a, b). The high correlation between the $r_{NP,NA}$ and PCI ($r = -0.79$) substantiates that the variability in the PCI during the winter AO pattern is primarily governed by the intensity of SPV and the resultant atmospheric coupling between the North Pacific and North Atlantic (Fig. 2a, b). The varied Pacific center of AO can also cause the AO to have a variable influence on the climate in western North America and East Asia. For East Asia, a larger PCI can lead to a more extensive warming of SAT in East Asia, even extending eastward into the North Pacific (Supplementary Fig. 2c). In contrast, under a weak PCI, the influence of the AO on winter SAT in East Asia is mainly confined to the East Asian continent (Supplementary Fig. 2d). For western North America, varying PCI can even induce opposite effects of the AO. A larger PCI of AO pattern during SSPV leads to cold SAT anomalies in the western North America due to the northwesterly anomalies on the eastern flank of a pronounced anticyclone (Supplementary Fig. 2c). Conversely, the negative SAT anomalies over western North America associated with the AO dissipate and shift to weak positive SAT anomalies during the WSPV phase with weak PCI (Supplementary Fig. 2d). This result suggests that the winter climate prediction or projection in East Asia and western North America associated with AO requires careful consideration of the potential significant impact of the changes in AO's Pacific center.

Time-varying AO's Pacific center essentially modulated by the AMO

Numerous studies have established that the multidecadal phase shifts of the AO/NAO are linked with the AMO[29–33], it raises a question: Could the AMO also impact the multidecadal variability of the AO's Pacific center? To investigate this, we regressed the winter SST anomalies onto the interdecadal component of the SPV index for the period 1958–2022. It reveals that the SST anomaly pattern in the North Atlantic, associated with the SPV, closely resembles the AMO-like SST anomaly pattern (Fig. 3a). A stronger SPV is generally associated with negative AMO-like SST anomalies extending from mid to high latitudes. Furthermore, the correlation coefficient of interdecadal components between the SPV and AMO indices during this period is −0.76 (Fig. 3b), exceeding 95% confidence level. We further extend the data from 1958 back to 1920 using the latest 20th-century reanalysis data (20CRv3) and found that the SPV and AMO also show a significant negative correlation ($r = -0.81$) over the longer period from 1920 to 2022 (Supplementary Fig. 3a), affirming the significant influence of the AMO on the SPV's strength and consequently on the Pacific center of the AO over interdecadal timescales.

It is observed that a poleward amplified negative SST anomaly pattern, associated with a negative phase of the AMO, can intensify the north-south temperature gradient from mid-latitudes to high latitudes. This enhancement potentially strengthens the zonal winds and the SPV through barotropic and baroclinic mechanisms[29,37]. To elucidate the impact of the AMO on the atmospheric circulation, we regressed the 100hPa zonal wind and zonal-mean zonal wind anomalies in the Northern Hemisphere against the interdecadal component of the reversed AMO index for the period 1958–2022. The results clearly show accelerated zonal winds (Fig. 3c) and a strengthened SPV (Fig. 3d) in response to the negative AMO, which can promote increased reflection of planetary waves from the North Pacific to the North Atlantic. This dynamic reflection, driven by the negative AMO, thus enhances the atmospheric coupling between the North Pacific and North Atlantic, significantly contributing to a pronounced Pacific center in the AO pattern (Fig. 4). The modulation of westerlies in the upper troposphere to the stratosphere at high latitudes by the AMO is also significant when using the longer data from 1920 to 2022 (Supplementary Fig. 3b). To substantiate the influence of AMO-related amplified SST anomalies over high latitudes on the SPV, two 20-member ensemble sensitivity experiments were conducted using the ECHAM5 atmospheric model. The control experiment (CTRL) utilized the boundary conditions of monthly SST climatology, whereas the sensitivity experiment (NAMO) incorporated negative AMO-related SST anomalies in the North Atlantic (0°–75°N, 0°–60°W) superimposed on the climatological SST. In response to amplified SST cooling over high latitudes associated with AMO, the strengthened zonal winds, SPV, and wave reflection are well reproduced, though at somewhat weaker magnitudes than observed (Supplementary Fig. 4a–c). The SLP differences between NAMO and CTRL experiments also show the positive AO-like pattern, with a weak but detectable Pacific center (Supplementary Fig. 4d). Some of the discrepancies in the ECHAM5 simulations are likely due to its limited ability to accurately replicate the atmospheric circulation's realistic response to SST forcing.

Response of SPV and AO's Pacific center to the AMO in CMIP6 models

Here we also use the historical simulations from 35 CMIP6 models for the period 1850–2014 to further verify the impacts of poleward amplification of

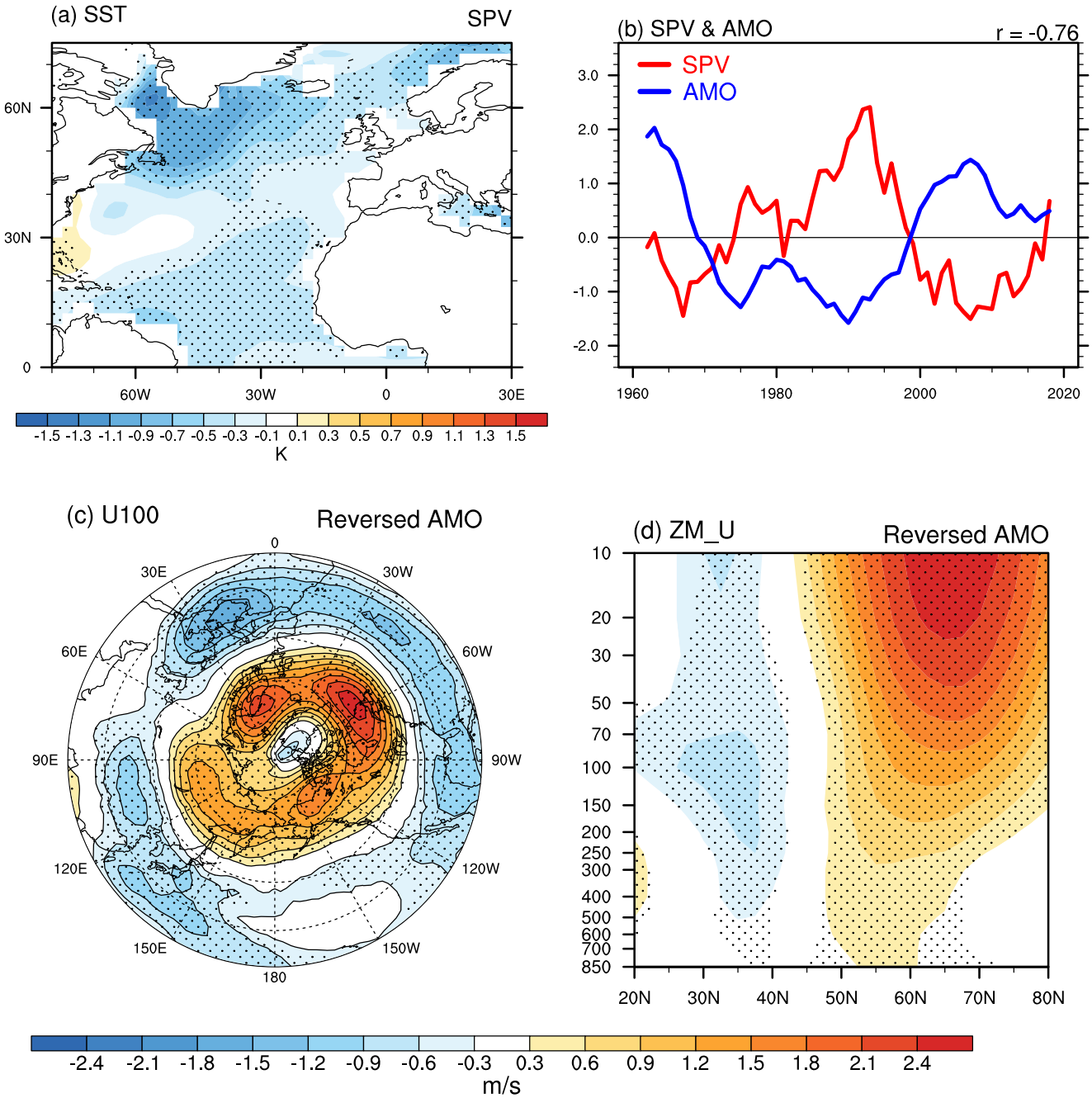

Fig. 3 | AMO modulating the strength of SPV. a The winter SST anomalies regressed on the interdecadal component of SPV index obtained using a 9-year low-pass filter during 1958–2022. **b** Temporal evolutions of interdecadal components of SPV (red line) and AMO (blue line) indices during 1958–2022. **c** 100hPa zonal wind (U100) anomalies regressed on the interdecadal component of AMO index during 1958–2022. **d** As in **c**, but for zonal-mean zonal wind (ZM_U) anomalies. Dots indicate the significance exceeding 95% confidence level.

AMO SST anomalies on SPV and Pacific center of AO. Figure 5 shows a scatterplot of the correlation coefficients between the AMO and SPV during 1850–2014 (Cor < AMO, SPV>) against the degree of poleward-amplified AMO SST anomalies in the North Atlantic. Here the degree of poleward amplification (PA) of AMO SST anomalies is defined as the differences in negative AMO-related SST anomalies between the low (15°–40°N, 70°–5°W) and high (45°–75°N, 65°W–20°E) latitudes in the North Atlantic. We found that although all models can simulate the negative correlation between the AMO and SPV, the negative correlation is significantly strengthened with the enhancement of the poleward amplified AMO SST anomalies. The inter-model correlation coefficient of Cor < AMO, SPV> with the degree of poleward amplified AMO SST anomalies among 35 CMIP6 models reaches −0.69, exceeding the 99.9% confidence level. This result supports that poleward amplified SST anomalies associated AMO can significantly enhance the response of the SPV to AMO.

To further validate the impact of the poleward amplified AMO SST anomalies on the zonal westerlies and SPV, we selected the eight models with the strongest (SPA) and weakest (WPA) poleward amplification of AMO SST anomalies for comparative analysis. In SPA models, compared to WPA models, we observe a stronger response of the SPV and the mid-to-high latitude westerlies to negative AMO SST anomalies (Fig. 6). The SLP anomalies associated with the AMO in the SPA and WPA models are displayed in Fig. 7a, b. Although a positive AO-like SLP response to the negative AMO can be seen both in SPA and WPA models, its intensity is

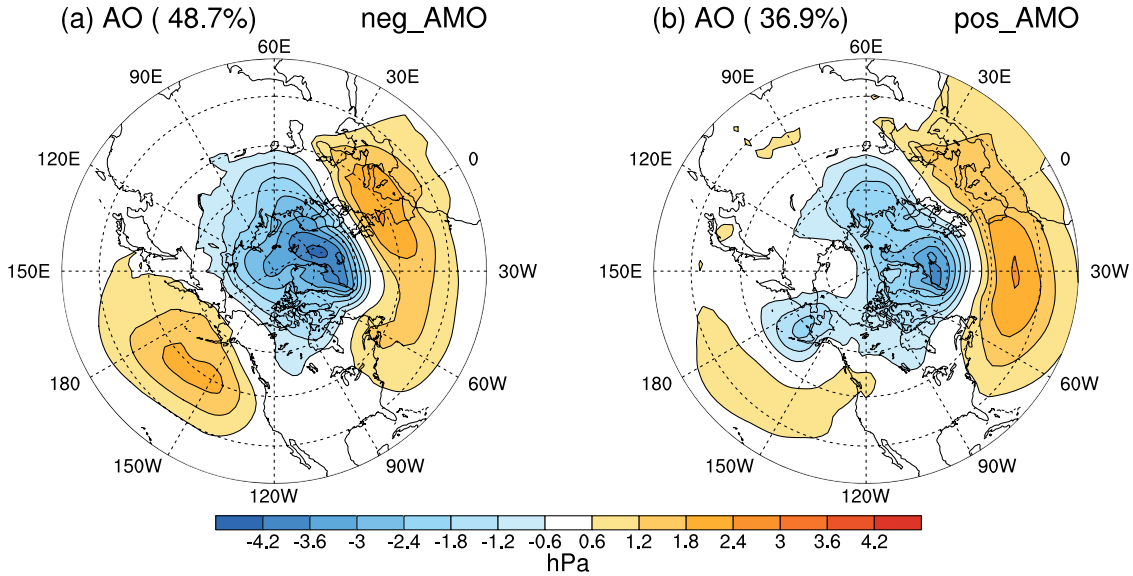

Fig. 4 | Winter AO pattern during the different phases of AMO. a First EOF mode of the SLP variability in the extratropical Northern Hemisphere during the negative phase of AMO (1970–1998). **b** As in **a**, but for positive phase of AMO (1958–1969 and 1999–2022).

noticeably stronger in the SPA models compared to the WPA models (Fig. 7a, b). Significant SLP anomalies in the North Pacific are observed only in the SPA models. Additionally, we further composite the AO pattern obtained from the first EOF mode of winter SLP in the extratropical Northern Hemisphere in both SPA and WPA models. It is clear that the Pacific center of the AO pattern is much stronger in SPA models than in WPA models (Fig. 7c, d). These results further confirm the conclusion drawn from observations and highlight the important role of poleward amplified AMO SST anomalies on the SPV and AO's Pacific center in both observations and CMIP6 models.

Discussion

This study elucidates the intricate dynamics underpinning the multidecadal variability of the AO's Pacific center, highlighting the pivotal role of the SPV in modulating the AO pattern, through its influence on the planetary wave reflection from the North Pacific to North Atlantic. This interaction is significantly influenced by the AMO, whose associated poleward amplified SST anomaly pattern changes the north-south thermal gradient in the mid- to high-latitude North Atlantic, thereby modulating the intensity of the westerlies, SPV, and related dynamical process markedly affecting the amplitude of the AO's Pacific center. This study not only advances our understanding of the mechanisms driving the variability of the AO pattern but also underscores the necessity of incorporating ocean-atmosphere interactions, particularly those involving the AMO, into climate predictions, which could significantly modulate the accuracy of AO-related regional climate projections.

In this study, we primarily explore the causes of the time-varying Pacific center of the AO pattern over the past decades. It is also worth noting that the Atlantic center of the AO is nonstationary as well and the positive SAT anomalies in the western coast of North America associated with AO during WSPV may be partly attributed to a stronger Atlantic center of the AO, particularly in its western segment, compared to the period of SSPV. We find that the variability in the amplitudes of the AO's Atlantic center is primarily linked to the variable amplitude of local SLP variability there (Supplementary Fig. 5a). A larger magnitude of SLP variability in the Atlantic (AVI) tends to correspond to a stronger Atlantic center (ACI) of AO pattern during 1958–2022 ($r = 0.73$). This suggests that the varied AO's Atlantic center is primarily modulated by the changes in the amplitude of North Atlantic SLP variability itself. Additionally, our analysis reveals no significant correlation ($r = 0.12$) between the local SLP variability in the North Pacific (PVI) and the PCI during 1958-2022 (Supplementary Fig. 5b). This result suggests that the reasons for the variability of the AO's Atlantic center are quite different from those of the AO's Pacific center. The question of what factors influence SLP variability in the North Atlantic warrants further research in the future.

Methods

Observational data

In this study, the monthly mean atmospheric variable proxies derived from the latest European Centre from Medium-Range Weather Forecast (ECMWF) Reanalysis v5 (ERA5) reanalysis, covering the period from January 1958 to present, with a spatial resolution of 1° × 1°[38]. The sea surface temperature (SST) data were from the NOAA Extended Reconstructed SST (ERSST) version 5 dataset[39], which has a horizontal resolution of 2° × 2° and covers the period from January 1854 to the present. The 20th-century reanalysis data (20CRv3)[40] is employed to extend the ERA5 data from 1958 back to 1920. This study focuses on the boreal winter months (December, January, and February), with "winter 1958" referring to the winter season of 1957/1958.

Definition of AO, AMO and SPV

The AO pattern is defined as the leading EOF mode of winter-mean sea-level pressure (SLP) variability across the extratropical Northern Hemisphere (20°–90°N) during 1958–2022, with the corresponding principal component (PC) representing the AO index[1]. The AMO index is defined as the area-averaged SST anomalies over the North Atlantic (0°–75°N, 60°W–0°). The 100-hPa zonal-mean zonal winds at 55°N are used to represent the strength of the SPV. The three-dimensional wave activity flux[41] is employed to trace the propagation of stationary planetary waves.

Definition of time-varying AO pattern

To examine variations in the AO pattern on decadal and longer timescales, the AO index is subjected to three-year moving averages before calculating the fluctuation of AO-related circulation[42]. To quantify the time-varying amplitudes of the AO pattern, the Pacific center intensity (PCI) and the Atlantic center intensity (ACI) of winter AO pattern were calculated using area-averaged SLP anomalies regressed onto 21-year sliding AO index over the North Pacific (25°–55°N, 125°E–135°W) and North Atlantic (20°–50°N, 90°W–30°E), respectively.

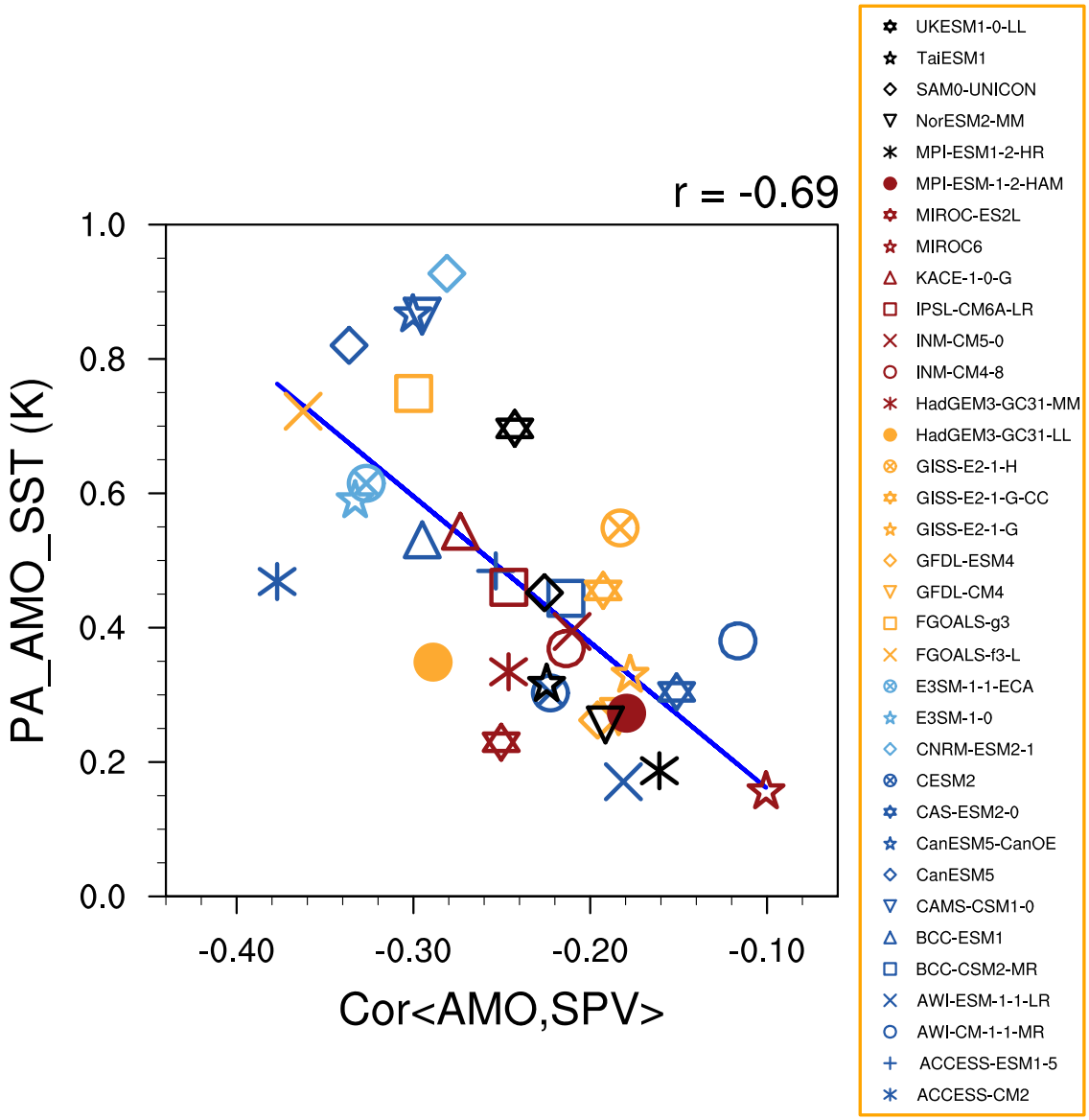

Fig. 5 | Relationship between AMO-SPV linkage and degree of poleward amplified AMO SST in 35 CMIP6 models. Scatterplot of the correlation coefficients between the AMO and SPV (Cor<AMO, SPV >) during 1850-2014 with the degree of poleward amplified AMO SST anomalies in the North Atlantic among 35 CMIP6 models.

Definition of time-varying magnitude of SLP variability

The time-varying magnitude of winter SLP variability in Pacific (PVI) and Atlantic (AVI) were defined as the area-averaged standard deviation of original winter SLP in the regions corresponding to the centers of AO in the North Pacific and North Atlantic, respectively, in a 21-year window during 1958–2022.

Definition of North Pacific-North Atlantic coupling

The correlation coefficient of SLP anomalies between the North Pacific region (25°–55°N, 125°E–135°W) and North Atlantic region (55°–80°N, 50°W–0°) was used to measure the linkage of the atmospheric circulation between the North Pacific and North Atlantic ($r_{NP,NA}$). This definition is similar to the Aleutian Low and Icelandic Low seesaw[35].

Model experiment

We use the atmospheric general circulation model of ECHAM, version 5 (ECHAM5) developed by the Max Planck Institute (MPI) for Meteorology[43] verify the influence of the AMO-related SST anomaly forcing on the zonal winds and SPV. The resolution of ECHAM5 model was T63 spectral triangular 63 (T63) and 19 vertical levels in a sigma pressure coordinate system. Two 20-member ensemble datasets were driven by the boundary conditions of monthly SST climatology (namely, CTRL) and negative AMO-related SST anomalies in the North Atlantic (0°–75°N, 0°–60°W) superimposed on the climatological SST (namely, NAMO), respectively. The imposed SST anomalies in the NAMO experiment are amplified by a factor of four to enhance the detectability of the atmospheric response at mid- and high latitudes.

CMIP6 simulations

The outputs of historical simulations for the period 1850–2014 are employed from 35 models from phase 6 of the Coupled Model Intercomparison Project (CMIP6) (Supplementary Table 1). We consider only the first realization from each CMIP6 model to maintain equal weighting across the models and all the model data were interpolated into the 2.5° × 2.5° longitude–latitude grid before analyses.

Data availability

The ERA5, ERSST v5, and 20CRv3 reanalysis data are available at: https://www.ecmwf.int/en/forecasts/dataset/ecmwf-reanalysis-v5, https://psl.noaa.gov/data/gridded/data.noaa.ersst.v5.html, and https://www.psl.noaa.gov/

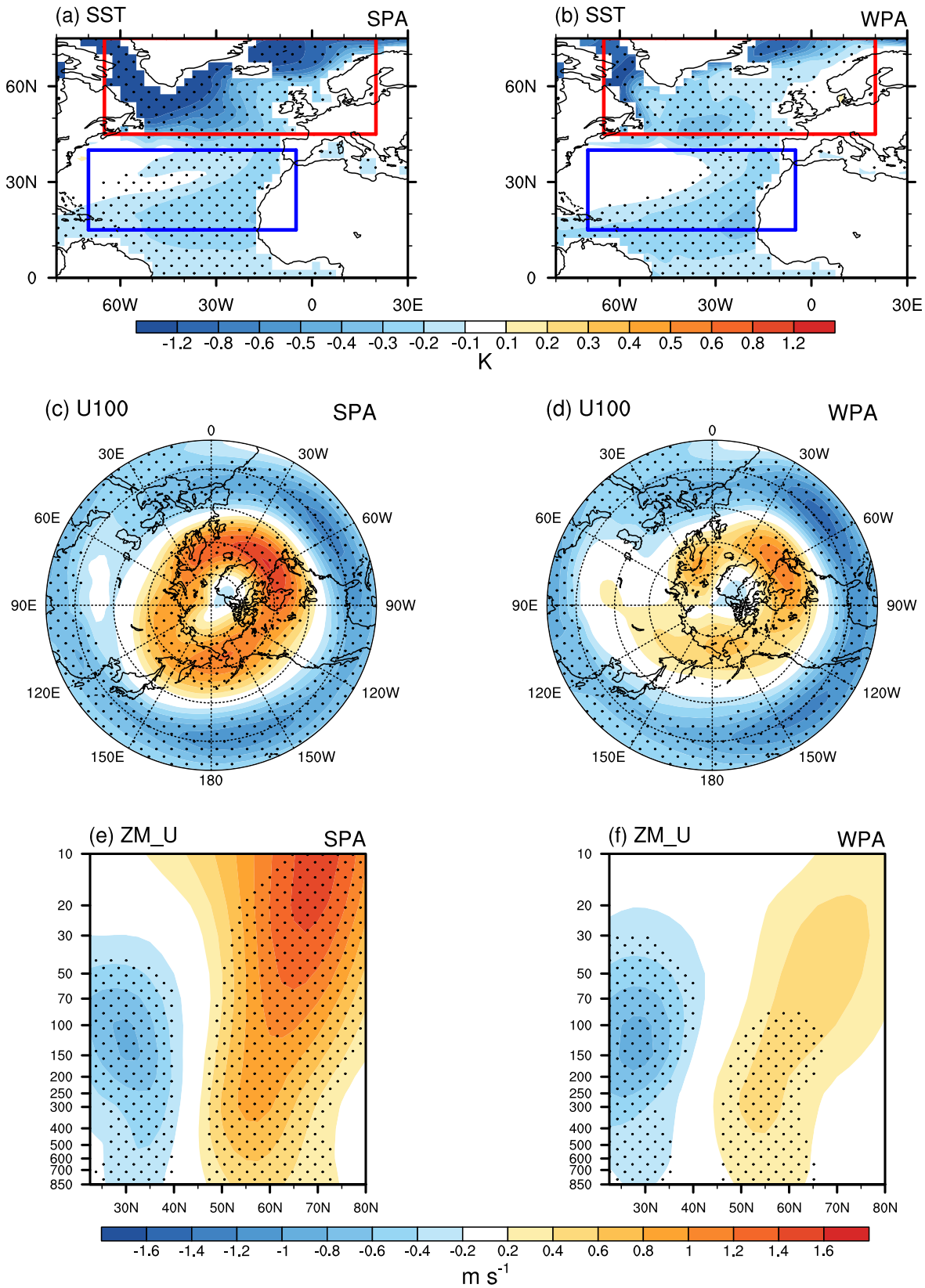

Fig. 6 | SPV and zonal winds responses to the AMO in SPA and WPA models. The winter SST anomalies regressed on the reversed AMO index during 1850–2014 in (**a**) SPA and (**b**) WPA models. **c**–**f** As in **a**, **b**, but for 100hPa zonal wind (U100) and zonal-mean zonal wind (ZM_U), respectively. Dots indicate the significance exceeding 95% confidence level. The blue and red boxes indicate the low-latitude and high-latitude regions used for the AMO SST anomalies, respectively.

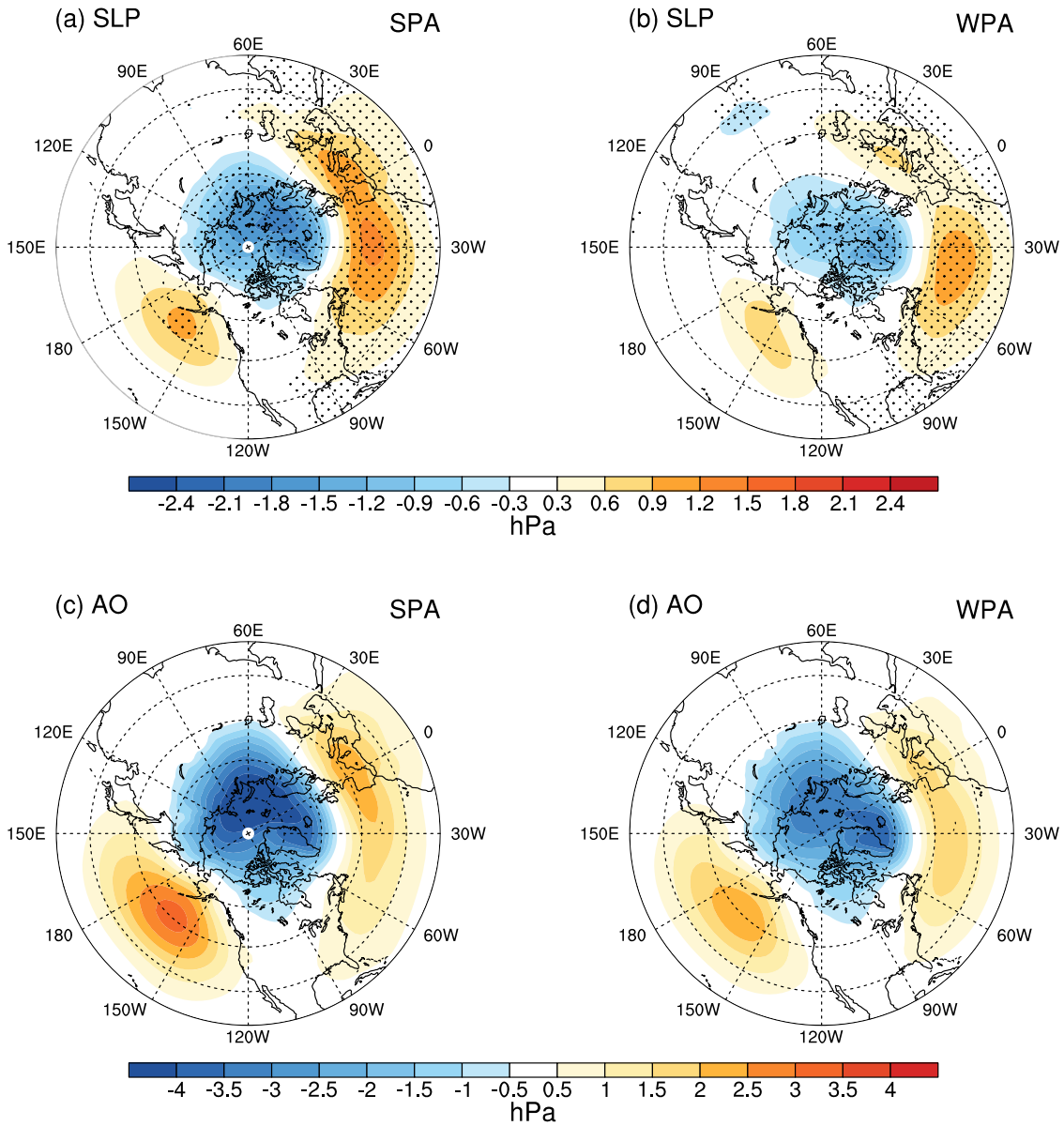

Fig. 7 | AMO-related SLP and AO pattern in the SPA and WPA models. The winter SLP anomalies regressed on the reversed AMO index during 1850–2014 in (**a**) SPA and (**b**) WPA models. **c**, **d** As in **a**–**b**, but for AO pattern. Dots indicate the significance exceeding 95% confidence level.

data/gridded/data.20thC_ReanV3.html, respectively. The CMIP6 simulations are available at https://esgf-node.llnl.gov/projects/cmip6/. The data of model experiment are available from the corresponding author on reasonable request.

Code availability

All figures in this paper are produced by the NCL, and the source codes can be obtained upon request to the first author.

Received: 23 May 2024; Accepted: 11 October 2024;
Published online: 27 October 2024

References

1. Thompson, D. W. J. & Wallace, J. M. The Arctic Oscillation signature in the wintertime geopotential height and temperature fields. *Geophys. Res. Lett.* **25**, 1297–1300 (1998).
2. Wallace, J. M. North Atlantic Oscillation/Annular Mode: Two paradigms-one phenomenon. *Q. J. R. Meteorological Soc.* **126**, 791–805 (2000).
3. Wallace, J. M. & Thompson, D. W. J. The Pacific Center of Action of the Northern Hemisphere Annular Mode: Real or Artifact? *J. Clim.* **15**, 1987–1991 (2002).
4. Deser, C. On the teleconnectivity of the "Arctic Oscillation". *Geophys. Res. Lett.* **27**, 779–782 (2000).
5. Baldwin, M. P. & Dunkerton, T. J. Stratospheric Harbingers of Anomalous Weather Regimes. *Science* **294**, 581–584 (2001).
6. Feldstein, S. B. & Franzke, C. Are the North Atlantic Oscillation and the Northern Annular Mode distinguishable? *J. Atmos. Sci.* **63**, 2915–2930 (2006).
7. Gong, H. et al. Biases of the wintertime Arctic Oscillation in CMIP5 models. *Environ. Res. Lett.* **12**, 014001 (2017).
8. Zhao, H. & Moore, G. W. K. Temporal variability in the expression of the Arctic Oscillation in the North Pacific. *J. Clim.* **22**, 3110–3126 (2009).
9. Shi, N. & Nakamura, H. Multi-decadal modulations in the Aleutian-Icelandic low seesaw and the axial symmetry of the Arctic Oscillation signature, as revealed in the 20th century reanalysis. *Tellus* **66A**, 22660 (2014).

10. Gong, H. et al. Multidecadal fluctuation of the wintertime Arctic Oscillation pattern and its implication. *J. Clim.* **31**, 5595–5608 (2018).
11. Thompson, D. W. J. & Wallace, J. M. Annular modes in the extratropical circulation. Part I: Month-to-month variability. *J. Clim.* **13**, 1000–1016 (2000).
12. Thompson, D. W. J. & Wallace, J. M. Regional climate impacts of the Northern Hemisphere annular mode. *Science* **293**, 85–89 (2001).
13. Cohen, J. et al. Winter 2009–2010: A case study of an extreme Arctic Oscillation event. *Geophys. Res. Lett*. **32**, L17707 2010.
14. Wang, L. & Chen, W. Downward Arctic Oscillation signal associated with moderate weak stratospheric polar vortex and the cold December 2009. *Geophys. Res. Lett.* **37**, L09707 (2010).
15. Gong, H. et al. Attribution of the East Asian winter temperature trends during 1979-2018: Role of external forcing and internal variability. *Geophys. Res. Lett.* **46**, 10874–10881 (2019).
16. Gong, H. et al. Time-varying contribution of internal dynamics to wintertime land temperature trends over the Northern Hemisphere. *Geophys. Res. Lett.* **46**, 14674–14682 (2019).
17. Castanheira, J. M. & Graf, H. F. North Pacific-North Atlantic relationships under stratospheric control? *J. Geophys. Res.-Atmosp.* **108**, ACL11-1–ACL11-10 (2003).
18. Sun, J. & Tan, B. Mechanism of the wintertime Aleutian Low–Icelandic Low seesaw. *Geophys. Res. Lett.* **40**, 4103–4108 (2013).
19. Perlwitz, J., et al. Large-scale circulation and climate variability. *In*: *Climate Science Special Report: Fourth National Climate Assessment*, Volume I [Wuebbles, D. J., D. W. Fahey, K. A. Hibbard, D. J. Dokken, B. C. Stewart, and T. K. Maycock (eds.)]. U.S. Global Change Research Program, Washington, DC, USA, pp. 161-184, https://doi.org/10.7930/J0RV0KVQ (2017).
20. Gong, H. et al. Diversity of the Wintertime Arctic Oscillation Pattern among CMIP5 Models: Role of the Stratospheric Polar Vortex. *J. Clim.* **32**, 5235–5250 (2019).
21. Riddle, E. et al. CFSv2 ensemble prediction of the wintertime Arctic Oscillation. *Clim. Dyn.* **41**, 1099–1116 (2013).
22. Kang, D. et al. Prediction of the Arctic Oscillation in boreal winter by dynamical seasonal forecasting systems. *Geophys. Res. Lett.* **41**, 3577–3585 (2014).
23. Siegert, S. et al. A Bayesian framework for verification and recalibration of ensemble forecasts: How uncertain is NAO predictability? *J. Clim.* **29**, 995–1012 (2016).
24. Hall, R. J. et al. Simple statistical probabilistic forecasts of the winter NAO. *Weather Forecast.* **32**, 1585–1601 (2017).
25. Ren, H. & Nie, Y. Skillful prediction of winter Arctic Oscillation from previous summer in a linear empirical model. *Sci. China Earth Sci.* **64**, 27–36 (2021).
26. Deser, C., Magnusdottir, G., Saravanan, R. & Phillips, A. The effects of North Atlantic SST and sea ice anomalies on the winter circulation in CCM3. Part II: Direct and indirect components of the response. *J. Clim.* **17**, 877–889 (2004).
27. Magnusdottir, G., Deser, C. & Saravanan, R. The effects of North Atlantic SST and sea ice anomalies on the winter circulation in CCM3. Part I: Main features and storm track characteristics of the response. *J. Clim.* **17**, 857–876 (2004).
28. Knight, J., Folland, C. & Scaife, A. Climate impacts of the Atlantic Multidecadal Oscillation. *Geophys. Res. Lett.* **33**, L17706 (2006).
29. Peings, Y. & Magnusdottir, G. Forcing of the wintertime atmospheric circulation by the multidecadal fluctuations of the North Atlantic Ocean. *Environ. Res. Lett.* **9**, 034018 (2014).
30. Peings, Y. & Magnusdottir, G. Wintertime atmospheric response to Atlantic multidecadal variability: Effect of stratospheric representation and ocean–atmosphere coupling. *Clim. Dyn.* **47**, 1029–1047 (2016).
31. Peings, Y., Simpkins, G. & Magnusdottir, G. Multidecadal fluctuations of the North Atlantic Ocean and feedback on the winter climate in CMIP5 control simulations. *J. Geophys. Res.-Atmospheres* **121**, 2571–2592 (2016).
32. Sun, C., Li, J. & Jin, F. A delayed oscillator model for the quasi-periodic multidecadal variability of the NAO. *Clim. Dyn.* **45**, 2083–2099 (2015).
33. Omrani, N.-E. et al. Stratosphere key for wintertime atmospheric response to warm Atlantic decadal conditions. *Clim. Dyn.* **42**, 649–663 (2014).
34. Charney, J. G. & Drazin, P. G. Propagation of planetary scale disturbances from the lower into the upper atmosphere. *J. Geophys. Res.* **66**, 83–109 (1961).
35. Honda, M. et al. Interannual Seesaw between the Aleutian and Icelandic Lows. Part I: Seasonal Dependence and Life Cycle. *J. Clim.* **14**, 1029–1042 (2001).
36. Honda, M. et al. Formation, Mechanisms, and Predictability of the Aleutian–Icelandic Low Seesaw in Ensemble AGCM Simulations. *J. Clim.* **18**, 1423–1434 (2005).
37. Nie, Y. et al. Delineating the Barotropic and Baroclinic Mechanisms in the Midlatitude Eddy-Driven Jet Response to Lower-Tropospheric Thermal Forcing. *J. Atmos. Sci.* **73**, 429–448 (2016).
38. Hersbach, H. et al. The ERA5 global reanalysis. *Q. J. R. Meteorological Soc.* **146**, 1999–2049 (2020).
39. Huang, B. et al. Extended reconstructed sea surface temperature, version 5 (ERSSTv5): upgrades, validations, and intercomparisons. *J. Clim.* **30**, 8179–8205 (2017).
40. Slivinski, L. et al. Towards a more reliable historical reanalysis: Improvements for version 3 of the Twentieth Century Reanalysis system. *Q. J. R. Meteorological Soc.* **145**, 2876–2908 (2019).
41. Takaya, K. & Nakamura, H. A Formulation of a Phase-Independent Wave-Activity Flux for Stationary and Migratory Quasigeostrophic Eddies on a Zonally Varying Basic Flow. *J. Atmos. Sci.* **58**, 608–627 (2001).
42. Dai, A. et al. Decadal modulation of global surface temperature by internal climate variability. *Nat. Clim. Change* **5**, 555–559 (2015).
43. Roeckner, E. et al. Sensitivity of simulated climate to horizontal and vertical resolution in the ECHAM5 atmosphere model. *J. Clim.* **19**, 3771–3791 (2006).

Acknowledgements

We thank the ECMWF and NOAA for making the ERA5 and ERSST v5 data and available for use. H.G., K.M., B.L. and L.W., were supported by the National Natural Science Foundation of China (41925020, 42075033, and 42275023) and the National Key R&D Program of China (2022YFE0106900). J.C. was supported by the US National Science Foundation grant AGS-2140909 and OPP-2115072.

Author contributions

L.W. conceived the study. H.G. performed the data analysis. H.G. and L.W. provided the interpretation and wrote the manuscript. J.C. helped improve the manuscript. K.M. and B.L. prepared the data and conducted the experiments. All authors discussed the results and contributed to writing the manuscript.

Competing interests

The authors declare no competing interests.

Additional information

Supplementary information The online version contains supplementary material available at https://doi.org/10.1038/s41612-024-00805-z.

Correspondence and requests for materials should be addressed to Lin Wang.